Deficiency of Ferritin Heavy-Chain Nuclear Import in Triple A Syndrome Implies Nuclear Oxidative Damage as the Primary Disease Mechanism

Helen L. Storr,* Barbara Kind,* David A. Parfitt, J. Paul Chapple, M. Lorenz, Katrin Koehler, Angela Huebner, and Adrian J. L. Clark

Centre for Endocrinology (H.L.S., D.A.P., J.P.C., A.J.L.C.), William Harvey Research Institute, Queen Mary University of London, Barts and the London School of Medicine and Dentistry, London EC1M 6BQ, United Kingdom; and Children's Hospital (B.K., K.K., A.H.), Technical University Dresden, and Max Planck Institute of Molecular Cell Biology and Genetics (M.L.), D-01307 Dresden, Germany

Triple A syndrome is a rare autosomal recessive disorder characterized by ACTH-resistant adrenal failure, alacrima, achalasia, and progressive neurological manifestations. The majority of cases are associated with mutations in the *AAAS* gene, which encodes a novel, 60-kDa WD-repeat nuclear pore protein, alacrima-achalasia-adrenal insufficiency neurological disorder (ALADIN) of unknown function. Our aim was to elucidate the functional role of ALADIN by determining its interacting protein partners using the bacterial two-hybrid (B2-H) technique. Nonidentical cDNA fragments were identified from both a HeLa S-3 cell and human cerebellar cDNA library that encoded the full-length ferritin heavy chain protein (FTH1). This interaction was confirmed by both co-immunoprecipitation and fluorescence lifetime imaging microscopy-fluorescence resonance energy transfer studies. Immunoblotting showed that fibroblasts from triple A patients (with known *AAAS* mutations) lack nuclear FTH1, suggesting that the nuclear translocation of FTH1 is defective. Cells transfected with *FTH1* and visualized by confocal microscopy had very little nuclear FTH1, but when cotransfected with *AAAS*, FTH1 is readily visible in the nuclei. Therefore, FTH1 nuclear translocation is enhanced when ALADIN is coexpressed in these cells. In addition to its well known iron storage role, FTH1 has been shown to protect the nucleus from oxidative damage. Apoptosis of neuronal cells induced by hydrogen peroxide was significantly reduced by transfection of *AAAS* or by *FTH1* or maximally by both genes together. Taken together, this work offers a plausible mechanism for the progressive clinical features of triple A syndrome. **(*Molecular Endocrinology* 23: 2086–2094, 2009)**

Triple A syndrome is an autosomal recessive disorder characterized by adrenal failure, achalasia of the cardia, alacrima (absence of tears), and a variety of progressive central, peripheral, and autonomic neurological defects (1). The spectrum of clinical manifestations is unique and encompasses a range of phenotypic abnormalities that can be highly heterogeneous even within affected families (2). The features of the disorder tend to be progressive, and the full clinical picture may develop over many years. No current therapies are available for the progressive neurological dysfunction, and the treatments for other aspects of triple A syndrome including the adrenal failure are aimed at symptom relief rather than prevention or cure (1, 3).

Adrenal hypofunction does not occur in the immediate postnatal period but at a variable time after this, suggesting progressive adrenal destruction or degeneration (4). Alacrima is the earliest and most consistent symptom of triple A syndrome and has been attributed to both autonomic dysregulation and structural abnormalities of the lacrimal gland (1, 4). The achalasia usually occurs within

ISSN Print 0888-8809 ISSN Online 1944-9917
Printed in U.S.A.

doi: 10.1210/me.2009-0056 Received February 4, 2009. Accepted September 4, 2009.
First Published Online October 23, 2009
* H.L.S. and B.K. contributed equally to this work.

Abbreviations: ALADIN, Alacrima-achalasia-adrenal insufficiency neurological disorder; B2-H, bacterial two-hybrid; CFP, cyan fluorescent protein; DAPI, 4′,6-diamidino-2-indole; EBV, Epstein-Barr virus; FL, flexible linker; FLIM, fluorescence lifetime imaging microscopy; FRET, fluorescence resonance energy transfer; FTH1, ferritin heavy chain protein; GFP, green fluorescent protein; NPC, nuclear pore complex; PARP, poly(ADP-ribose) polymerase; YFP, yellow fluorescent protein.

the first two decades of life and may precede the adrenal failure by several years (1, 4). A highly variable, progressive neurological dysfunction tends to develop later in the disease and is present in approximately 60% of patients (3, 4). This neurodegenerative process affects the central, peripheral, and autonomic nervous systems (4).

Defects in the *AAAS* gene are responsible for approximately 82% of cases of triple A syndrome. The *AAAS* gene encodes a 60-kDa WD-repeat protein of unknown function, named ALADIN (alacrima-achalasia-adrenal insufficiency neurological disorder) (5, 6). There is little phenotype/genotype correlation, even between affected siblings, suggesting that other factors are involved in disease progression (2, 7). The presence of WD-repeats (producing a β-propeller structure) suggests that ALADIN is likely to be involved in protein-protein interactions and may mediate the assembly of multimolecular complexes (8).

AAAS is widely expressed (7, 9), and its protein product was identified as a component of the nuclear pore complex (NPC) (10, 11). ALADIN resides at the cytoplasmic face of the NPC, but *AAAS* mutations do not result in structural defects of the NPC (12). Many disease-associated missense, nonsense, and frameshift *AAAS* mutations result in ALADIN mislocalization, but the precise functional roles of ALADIN at the nuclear pore remain obscure (12, 13). Therefore, triple A syndrome may result from a tissue-specific failure of NPC function, but the mechanism of this complex and variable disease is unclear. Although several nucleoporins have been associated with specific human diseases, ALADIN remains the first nuclear pore protein responsible for a complex disease process due to a single gene defect.

In an attempt to determine the role of ALADIN, the full-length protein was used as bait in a bacterial two-hybrid (B2-H) screen of human cDNA libraries. We report a novel interacting protein partner for the nuclear pore protein ALADIN. Our findings also support the hypothesis that the cellular destruction in triple A syndrome is a result of oxidative damage and offers a plausible disease mechanism for the pathogenesis of this complex, degenerative disorder.

Results

Identification of ferritin heavy chain protein (FTH1) as an interacting protein partner for ALADIN

For B2-H screens, control cotransformation reactions were performed in accordance with the manufacturer's guidelines, which confirmed the expected results and the stringency of the system. Two screens of approximately 10^6 independent cDNA clones were performed, and non-identical cDNA fragments were isolated from both libraries. DNA sequencing revealed both to be homologous to the full-length coding region of human FTH1. The *FTH1* sequence was in-frame in each clone isolated and predicted to encode the full-length FTH1 protein. The pTRG-*FTH1* target was verified as a true positive interactor in the B2-H system by its growth on selective screening medium when it was retransformed with the pBT-*AAAS* bait vector and its failure to grow on selective screening medium when cotransformed with the empty pBT vector. Subsequent studies were directed toward validating the interaction of FTH1 and ALADIN.

Co-immunoprecipitation of FTH1/ALADIN in SK-N-SH cells

To verify the association of FTH1 and ALADIN, co-immunoprecipitation assays were performed. SK-N-SH neuroblastoma cells were cotransfected with green fluorescent protein (GFP)-ALADIN (pEGFP-*AAAS*) and wild-type (WT) FTH1 (pcDNA3.1-*FTH1*) (Fig. 1A) or polyhistidine-V5-tagged FTH1 (pcDNA3.1-*FTH1*-V5-HIS) vectors (Fig. 1B). Anti-GFP antibody immunoblot-

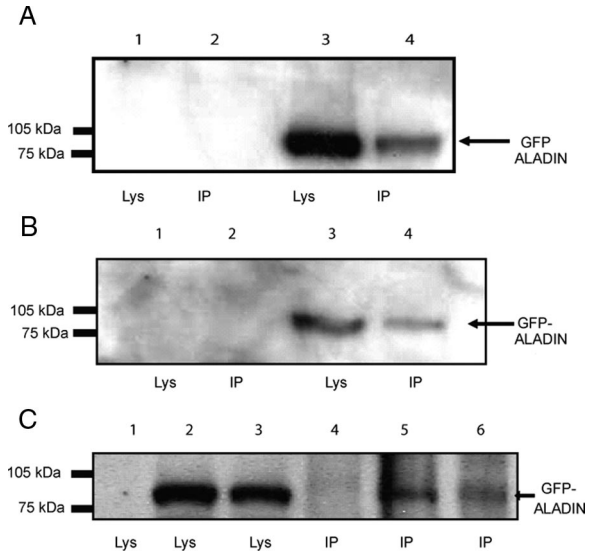

FIG. 1. Co-immunoprecipitation of the ALADIN-FTH1 complex in SK-N-SH cells. A, Co-immunoprecipitation assays were performed on SK-N-SH cells coexpressing GFP-ALADIN and FTH1. GFP-ALADIN is detected by immunoblotting using anti-GFP antibody and is readily detectable in non-immunoprecipitated cell lysate (Lys, lane 3) and in lysates immunoprecipitated with anti-FTH1 (IP, lane 4) but not in cell lysate or immunoprecipitates of cells transfected with pcDNA 3.1 alone (lanes 1 and 2). B, Co-immunoprecipitation assays were performed on SK-N-SH cells coexpressing GFP-ALADIN and V5-His-tagged FTH1. GFP-ALADIN is detected by immunoblotting using anti-GFP antibody and is readily detectable in non-immunoprecipitated cell lysate (lane 3) and in lysates immunoprecipitated with anti-6XHis (lane 4) but not in cell lysate or immunoprecipitates of cells transfected with pcDNA 3.1 alone (lanes 1 and 2). C, Co-immunoprecipitation assays were performed on SK-N-SH cells transfected with empty vector alone or expressing GFP-ALADIN and/or FTH-1 as indicated. Anti-FTH1 antibody co-immunoprecipitates both induced FTH1 or endogenously expressed FTH1 and GFP-ALADIN (lanes 5 and 6). Molecular weight marker positions are indicated on the *left*.

ting identified the presence of GFP-ALADIN (90 kDa) after the immunoprecipitation of FTH1 with anti-FTH1 antibody (Fig. 1A, lane 4). Similarly, immunoprecipitation of FTH1-V5-His with the anti-6XHis antibody also enabled GFP-ALADIN to be identified on immunoblotting (Fig. 1B, lane 4). In the absence of transfected FTH1, endogenous FTH1 could also immunoprecipitate GFP-ALADIN (Fig. 1C, lane 6). This confirmed that the interaction was not dependent on the expression of supraphysiological amounts of FTH1 protein. Comparable data were obtained in HEK293 cells (data not shown).

Fluorescence lifetime imaging microscopy (FLIM)-fluorescence resonance energy transfer (FRET) analysis of FTH1/ALADIN in HeLa cells

To confirm the interaction of FTH1 and ALADIN *in vivo*, we performed FRET measurements. FRET was detected by FLIM. If FRET occurs, the donor lifetime decreases. All FLIM-FRET experiments were done in HeLa cells, which stably expressed cyan fluorescent protein (CFP)-ALADIN. The fluorescence lifetime of CFP was calculated in two different ways: 1) by a pixel-by-pixel approach with a single exponential decay function to generate a lifetime image (Fig. 2, A–C) and 2) by a cell-based approach, where an average decay curve was analyzed by a biexponential decay function (Fig. 2D). Although the shorter lifetime seems to be unchanged, the longer lifetime decreases in the case of FRET as observed previously (14, 15). To compare the results with the pixel-by-pixel analysis, we calculated the weighted mean lifetime τ_m.

The lifetime of CFP-ALADIN decreases from 2.63 ± 0.02 nsec (SEM; n = 44 pictures) to 2.55 ± 0.04 nsec (19 pictures) in the presence of FTH1-yellow fluorescent protein (YFP) on the image-based algorithm and from 2.63 ± 0.11 nsec (SD; n = 78 cells) to 2.40 ± 0.17 nsec (n = 121 cells) for the whole-cell analysis, respectively (Table 1 and Fig. 2D). The reduction of the lifetime clearly indicates a close proximity of both proteins. For comparison, the results of the analysis of the combination of CFP-ALADIN with the C-terminal YFP-tagged nucleoporin NUP88 as a negative control are also shown. NUP88 is a recognized component of the nuclear pore complex but does not seem to interact with ALADIN (16). In the case of NUP88, no decrease of the CFP lifetime was observed. The lifetimes were 2.63 ± 0.02 nsec (SEM; n = 11 pictures) in the pixel-by-pixel analyses and 2.61 ± 0.10 nsec (SD; n = 85 cells) in the whole-cell analysis (Table 1 and Fig. 2D). It is well recognized that ALADIN is normally localized to the nuclear membrane (10, 11), but instrumental limitations and the low fluorescence intensity of CFP-labeled ALADIN combined with the inevitable overexpression of transfected components makes it difficult to demonstrate conclusively that this interaction takes place only at the nuclear pore.

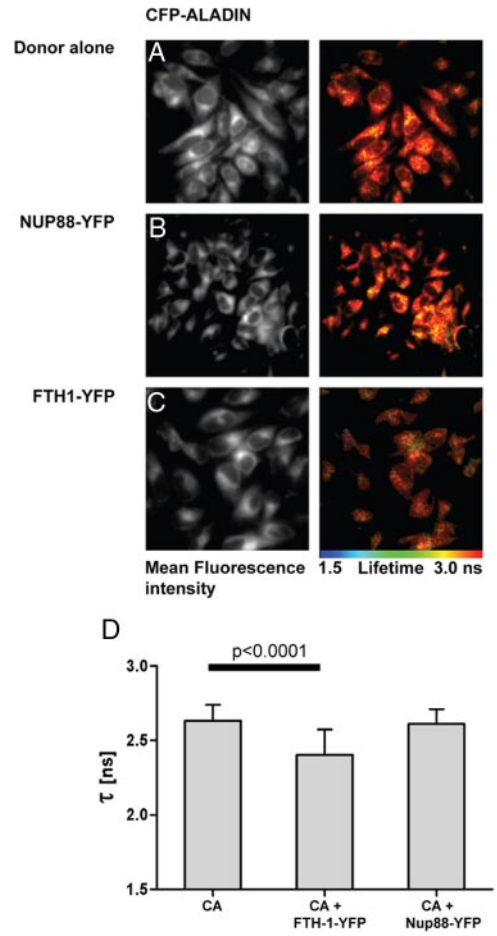

FIG. 2. HeLa cells stably expressing CFP-ALADIN only (A), transiently transfected with NUP88-YFP (B), or transiently transfected with FTH1-YFP (C). On the *left*, the CFP-ALADIN fluorescence intensity is shown, and on the *right*, the corresponding fluorescence lifetime is shown. A decrease of CFP-ALADIN lifetime is observed only in the presence of FTH1-YFP, whereas the lifetime in the presence of NUP88-YFP remains unchanged. D, Quantitative analysis of these data shows the mean lifetime of CFP-ALADIN (CA) in the absence and presence of FTH1-YFP or NUP88-YFP, respectively. The lifetime was significantly lower in the presence of FTH1-YFP and remained unchanged in the negative control with NUP88-YFP. *Error bars* are SD.

The nuclear translocation of FTH1 is dependent on the presence of ALADIN

The possibility that ALADIN might be involved in the nuclear translocation of FTH1 was investigated by immunoblotting of cytosolic and nuclear cell fractions. Cytosolic and nuclear extracts were prepared from cultured control fibroblasts ($ALADIN^{WT}$) and three fibroblast cell lines derived from triple A patients ($ALADIN^{Mut}$) homozygous for the following ALADIN mutations: IVS14+1G→C, p.S263P, and p.Q387X. Cytosolic and nuclear extracts were also prepared from cultured control Epstein-Barr virus (EBV)-transformed lymphocytes ($ALADIN^{WT}$) and one EBV-transformed lympho-

TABLE 1. Statistical analysis

	τ_1 (nsec)	τ_2 (nsec)	x_1[a]	τ_m (nsec)
Donor only (CFP-ALADIN)	3.61 ± 0.09	0.47 ± 0.03	0.23 ± 0.04	2.63 ± 0.11
CFP-ALADIN + FTH1-YFP	3.44 ± 0.11	0.46 ± 0.05	0.44 ± 0.14	2.40 ± 0.17
CFP-ALADIN + NUP88-YFP	3.63 ± 0.11	0.46 ± 0.02	0.21 ± 0.03	2.61 ± 0.10

For CFP-ALADIN alone and in combination with FTH1-YFP, the exact parameters of the double-exponential fitted decay curves are displayed. The negative FLIM-FRET result of the analysis of the combination CFP-ALADIN and NUP88-YFP is included in this table for comparison.

[a] $x_1 = A_1/(A_1+A_2)$.

cyte cell line derived from a triple A patient (ALADIN^{Mut}) heterozygous for the following ALADIN mutations: H71fs and R230X. Nuclear FTH1 was readily detectable by anti-FTH1 antibody in control cells (Fig. 3A, *panel* 1, and supplemental Fig. 1, *panel* 1, published as supplemental data on The Endocrine Society's Journals Online web site at http://mend.endojournals.org), whereas no nuclear FTH1 band is apparent in any of the triple A fibroblasts (Fig. 3A, *panels* 2–4) or the triple A EBV-transformed lymphocytes (supplemental Fig. 1, *panel* 2). Immunoblotting the triple A fibroblast and EBV-transformed lymphocyte nuclear extracts with anti-Nup 62 confirmed a band consistent with the Nup 62 protein (62 kDa) and therefore the presence of nuclear material in these samples (Fig. 3A, *panel* 5, and supplemental Fig. 1, *panel* 3).

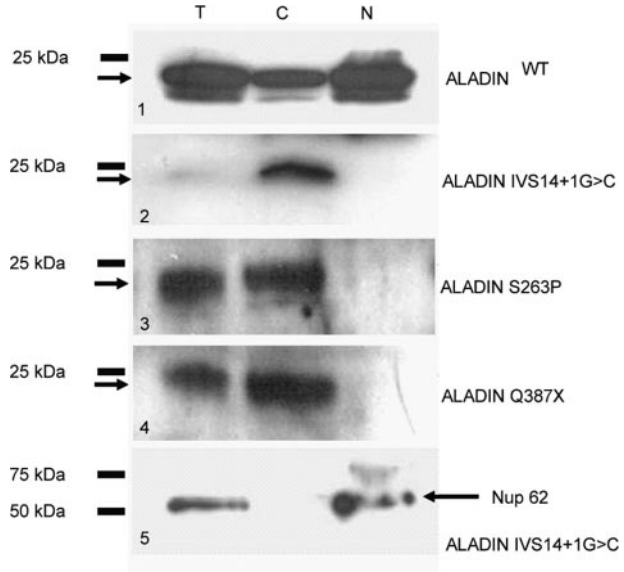

FIG. 3. Immunoblots of wild-type (ALADIN^{WT}) and triple A (ALADIN^{Mut}). FTH1 is detected by immunoblotting using anti-FTH1 antibody in ALADIN^{WT} and ALADIN^{Mut} fibroblast cell lysates. C, Cytoplasmic fraction; N, nuclear fractions; T, total cell lysate. Nuclear FTH1 is detectable (*arrows*; 21 kDa) in *panel* 1 (ALADIN^{WT}) but not in triple A (ALADIN^{Mut}) fibroblast cell lysates (*panel* 2, ALADIN IVS14+1G→C; panel 3, ALADIN p.S263P or panel 4, ALADIN p.Q387X). The ALADIN IVS14+1G→C fibroblast immunoblot (*panel* 2) stripped and re-immunoblotted with anti-Nup 62 antibody (nuclear marker, *arrow*; 62 kDa) confirms the presence of nuclear material in the ALADIN^{Mut} cell lysates (*panel* 5).

When SK-N-SH cells were transfected with pcDNA3.1-*FTH1*-V5-HIS and imaged by confocal microscopy, very little nuclear immunofluorescence was seen (Fig. 4, B–D). When SK-N-SH cells were cotransfected with both pcDNA3.1-*FTH1*-V5-HIS and pEGFP-*AAAS* vectors, FTH1 was readily visible in the nucleus (Fig. 4, F–H). Examination of several images by an independent observer indicated that zero of 22 transfected cells showed obvious nuclear localization in the absence of ALADIN, whereas 52 of 76 transfected cells showed evidence of nuclear FTH1 in the presence of ALADIN. This provides supportive evidence that the nuclear translocation of FTH1 is dependent on the presence of ALADIN.

FTH1 and ALADIN are protective against oxidative stress

To test whether increased FTH1 in the nucleus could protect against oxidative stress induced by exogenous hydrogen peroxide, neuroblastoma cells were transfected with pEGFP-*AAAS*, pcDNA3.1-*FTH1* or pEGFP-*AAAS* and pcDNA3.1-*FTH1* and subjected to an acute hydrogen peroxide stress. Poly(ADP-ribose) polymerase (PARP) was used a marker of apoptosis via immunoblot analysis. PARP cleavage from a full-length protein of 116- to 85-kDa and 27-kDa fragments is a well-documented effect of cell death by apoptosis (17, 18).

Untransfected cells treated with 1 mM hydrogen peroxide showed a marked increase in cleaved PARP relative to untreated controls (Fig. 5, Western blot). Cells cotransfected with pEGFP-*AAAS* and pcDNA3.1-*FTH1* showed a significant decrease in the amount of cleaved PARP relative to untransfected cells. Interestingly, transfection of pEGFP-*AAAS* or pcDNA3.1-*FTH1* alone also significantly reduced the relative amounts of cleaved PARP.

Discussion

The triple A syndrome is a rare, poorly understood, and highly disabling disease. Thus far, the molecular mechanism of this complex disorder resulting from mutations in a protein of unknown function named ALADIN has remained obscure (5, 6). Our results suggest that ALADIN

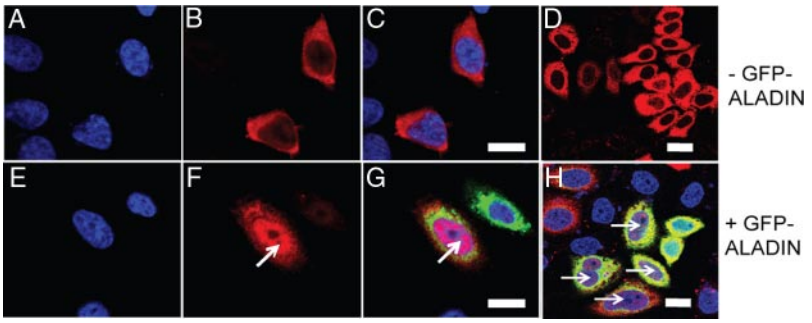

FIG. 4. FTH1-V5-His localizes to the nucleus in cotransfected SK-N-SH cells. SK-N-SH cells were either transfected with the pcDNA3.1-*FTH1*-V5-His vector alone (A–D) or cotransfected with the pcDNA3.1-*FTH1*-V5-His and pEGFP-*AAAS* vectors (E–H). Cells were incubated with the primary (anti-V5) antibody followed by the secondary (antimouse Cy3) antibody and visualized by laser scanning confocal microscopy. Images show the localization of DAPI nuclear stain (*blue*, A and E) and localization of the V5-His-tagged FTH1 (*red*, B and F). The merged DAPI/V5-His-tagged FTH1 image is shown in a single cell (C) and a population of cells (D).The merged DAPI/V5-His-tagged FTH1/GFP-tagged ALADIN image is shown in a single cell (G) and a population of cells (H). The V5-His-tagged FTH1 has a mainly cytoplasmic localization when transfected alone (B–D) but is clearly visualized in the nucleus when coexpressed with GFP-ALADIN (F–H) (*arrows*). Images are 73.1 × 73.1 μm. *Scale bars*, 10 μm.

interacts with and is involved in the nuclear translocation of FTH1. This provides a plausible disease mechanism for triple A syndrome because ALADIN deficiency, either because the protein is incomplete or because it fails to localize correctly to the nuclear pores, results in impaired FTH1 nuclear uptake, rendering cells more susceptible to oxidative damage.

FTH1 was identified as a partner protein for ALADIN by independent screens of two cDNA libraries. This interaction was reproducibly verified *in vivo* by co-immunoprecipitation and photobleaching FRET assays. FTH1 has a well established role as an iron-storage protein and is classically found in the circulating blood plasma or in the cytoplasmic fraction of the cell. An emerging body of evidence suggests that FTH1 is also present in the nucleus where it has a DNA-protective role (19–24). Ferrous iron catalyzes the conversion of reactive oxygen species into free radicals (the Fenton reaction), and consequently, free iron in the nucleus exacerbates oxidative and UV-induced DNA damage (25). Free iron has been shown to induce DNA nicks and single-strand breaks, but in the presence of FTH1, this activity is retarded (23). In astrocytoma cells, FTH1 associates closely with DNA, preventing cellular damage due to oxidative stress (24), and in corneal epithelial cells, nuclear FTH1 protects against iron and UV-induced oxidative damage (20, 21). The nuclear import of FTH1 is an active, importin-independent process via the NPC (19). This process is poorly defined except in the corneal epithelium where a nuclear import mechanism has been identified involving a ferritin-related protein, ferritoid, which contains a simian virus 40-type nuclear localization signal (22). However, this mechanism appears to be highly specific to this cell type (21–23).

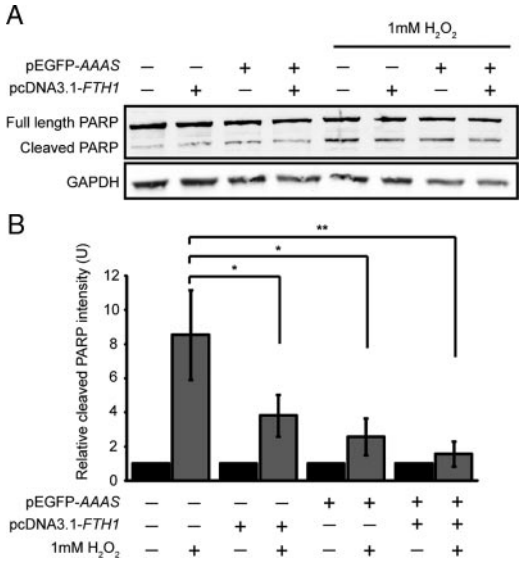

FIG. 5. FTH1 and ALADIN are protective against oxidative stress. A, Western analysis of SH-SY5Y cells transfected with pEGFP-*AAAS*, pcDNA3.1-*FTH1*, or pEGFP-*AAAS* and pcDNA3.1-*FTH1* and treated with or without hydrogen peroxide. Hydrogen peroxide treatment causes an increase in PARP cleavage relative to untreated controls, and cotransfection of pEGFP-*AAAS* and pcDNA3.1-*FTH1* reduces the amount of PARP cleavage relative to untransfected cells. B, Densitometric analysis showed a significant ($P = 0.01$) decrease in cleaved PARP between untransfected cells and cells cotransfected with pEGFP-*AAAS* and pcDNA3.1-*FTH1*. Values are intensities of cleaved PARP relative to GAPDH relative to untreated controls (*dark bars*). *, $P < 0.05$; **, $P < 0.01$; n = 4.

Ferritin heavy chain protein was found to be absent in the nuclei of fibroblasts isolated from triple A patients, and the nuclear translocation of FTH1 appears to be facilitated when it is coexpressed with ALADIN. These data support the possibility that ALADIN (which bears no structural homology to ferritoid) might be involved in the nuclear translocation of FTH1. ALADIN has no nuclear localization signal, and there is little evidence that it crosses the nuclear membrane as other nuclear transporters such as importins or ferritoid do (12). Thus, it seems very probable that other components are required for the successful uptake of FTH1, and this may relate to the small number of cases of triple A syndrome that are not associated with *AAAS* mutations (7, 13). It is possible that ALADIN may be involved in the nuclear translocation of other cargoes, although no other consistent hits were identified in our B2-H screens. It is surprising that no other nucleoporins were identified by the B2-H screening, because ALADIN should be incorporated into the NPC

by protein-protein interactions. This may represent a false-negative result of the B2-H. However, in humans, ALADIN undoubtedly undertakes a critical functional role at the NPC, and FTH1 also appears to have a fundamental function in the nuclear compartment (12, 13, 21, 23).

An intriguing question is why the triple A syndrome affects such a specific combination of tissues. One possibility is that certain tissues have a greater inherent susceptibility to the type of oxidative damage that ALADIN protects against compared with those tissues that are not affected. Alternatively, it may be that there are other FTH1 transport mechanisms active in those unaffected tissues such that ALADIN is redundant. Certainly, the central nervous system is particularly vulnerable to oxidative stress (25), and oxidative damage contributes to the progressive adrenal cortex destruction of X-linked adrenoleukodystrophy (26). The adrenal cortex is rich in mitochondria, and redox changes in adrenal cells were used as the basis of the original bioassays for ACTH.

It is also possible that ALADIN has other functional roles or that other DNA-protective mechanisms exist in parallel in some cell types. The fact that the *Aaas* knockout mouse exhibits a minimal phenotype might also reflect a lack of exposure to oxidative stress or the presence of murine proteins or transporters other than ALADIN that are responsible for these protective processes (27).

A higher frequency of chromosomal breakages is observed in triple A patients, which may indicate that the cells are more susceptible to free-radical-induced damage (28). Hirano and colleagues (29, 30) showed that cultured fibroblasts from a triple A syndrome patients were more sensitive to oxidative stress than control fibroblasts. Here we are able to confirm that oxidative stress in the form of exposure to hydrogen peroxide leads to increased PARP cleavage and that this is significantly reduced by overexpression of *AAAS* or *FTH1* or both. In summary, our work provides consistent evidence that oxidative stress is involved in the triple A syndrome disease progression. ALADIN may bind FTH1 alone or as part of a complex and assist the nuclear import of FTH1. Alternatively, it may be involved in the association or dissociation of the FTH1 nuclear transport complex.

The neurological phenotype of triple A syndrome has been compared with that of amyotrophic lateral sclerosis (31). It is notable that mutations of superoxide dismutase (SOD1), an important cellular antioxidant enzyme, have been identified in cases of familial amyotrophic lateral sclerosis (32). Oxidative damage has been implicated in the pathogenesis of other neurodegenerative disorders including Alzheimer's, Parkinson's, and Huntingdon's diseases (33). Furthermore, mice that are heterozygous (+/−) for a *FTH1* null mutation have evidence of increased oxidative damage to the central nervous system and provide a useful model of neurodegenerative diseases (25). All the major characteristic symptoms of triple A syndrome can exhibit clinical progression (1, 4, 7). This well-recognized feature of the disorder would be highly consistent with an ongoing process of cellular destruction secondary to oxidative damage. This pathogenic mechanism would also be consistent with the highly heterogeneous nature of the syndrome in which even siblings with the same *AAAS* mutations may have entirely discordant clinical findings (7, 34). Furthermore, antioxidant therapies, which are being considered as therapeutic options in other neurodegenerative disorders, might be valuable as interventions to prevent or slow disease progression in triple A syndrome (33, 35).

Materials and Methods

B2-H screens

B2-H screens were performed and positive interactors were identified as described previously (36). The full-length human ALADIN coding region was used as a bait fused by a $(Gly_4Ser)_3$ repeat flexible linker (FL) to the bacteriophage λ-cl repressor protein (λcI). The complete sequence and frame of the recombinant pBT-*AAAS* bait vector were verified by DNA sequencing. It was hypothesized that the protein partners interacting with ALADIN would be prevalent in the same tissues and cell lines as ALADIN. The pBT-*AAAS* bait vector was used to screen a human HeLa S-3 cell cDNA library and a human cerebellar cDNA library (Stratagene, Amsterdam, The Netherlands). Interactors that were out of frame and/or contained in-frame stop codons were treated as false positives and discarded from further investigations.

Construction of recombinant vectors

The full-length human ALADIN coding sequence was subcloned into the following two vectors from Invitrogen (Paisley, UK): pCR2.1 (pCR2.1-*AAAS*) and pEGFP-C1 (pEGFP-*AAAS*). For the construction of the pBT-*AAAS* bait vector, the ALADIN sequence was PCR-amplified from pCR2.1-*AAAS*, the forward primer incorporated the sequence encoding a FL $(Gly_4Ser)_3$. The PCR-amplified FL-*AAAS* was then subcloned into the pGEMT Easy cloning vector (Promega, Southampton, UK). The full-length human coding sequences of *AAAS* (with the 5′-FL sequence) and *FTH1* were PCR amplified from pGEMT-FL-*AAAS* and human adrenal cDNA, respectively, using primers incorporating an *Eco*RI restriction enzyme site at the 5′ end of the forward primer and an *Xho*I site at the 5′ end of the reverse primer. The *AAAS* and *FTH1* sequences were then cloned into the *Eco*RI and *Xho*I restriction enzyme sites of pBT bait plasmid (Stratagene) to produce the pBT-*AAAS* vector and pcDNA3.1 and pcDNA3.1/V5-His-TOPO (Invitrogen) to produce the pcDNA3.1-*FTH1* and pcDNA3.1-*FTH1*-V5-HIS vectors, respectively. All constructs were verified by DNA sequencing, and all primer sequences are available on request.

Cell culture, transfection, and immunodetection

Human control and patient fibroblast cells were used as they have been used in other similar studies and appear to be a good model system for the disease (29). SK-N-SH and fibroblast cells were cultured in 50% F-10 Nutrient Mixture (Ham) (GIBCO, Paisley, UK) and 50% DMEM (Sigma Chemical Co., St. Dorset, UK) or 100% MEM (GIBCO), respectively. EBV-transformed lymphocytes were cultured in RPMI 1640 medium. All media were supplemented with 10% fetal bovine serum and 1% penicillin/streptomycin solution, and the cells were incubated in a humidified incubator at 37 C and 5% CO_2. Total cell lysates and cytoplasmic and nuclear fractions were prepared as described (36).

SK-N-SH cells were grown to approximately 50–70% confluency before transfection using FuGENE 6 (Roche, Burgess Hill, UK) according to the manufacturer's protocol. Cells were either transfected with pcDNA 3.1 (control transfection) or pEGFP-*AAAS* alone or cotransfected with pEGFP-*AAAS* and pcDNA3.1-*FTH1*-V5-HIS or pEGFP-*AAAS* and pcDNA3.1-*FTH1*. Total cell lysates were prepared 48 h after transfection and incubated overnight with rotation at 4 C with 2.5 μg anti-FTH1 rabbit polyclonal antibody (AbCam, Cambridge, UK) or Anti-6XHis tag mouse monoclonal antibody (AbCam) before adding 50 μl Trueblot rabbit or mouse immunoprecipitation beads (eBioscience, Hatfield, UK), respectively. Samples were incubated for 2 h at room temperature with rotation and then centrifuged at top speed for 1 min and the supernatant removed. The beads were washed with 500 μl PBS three times and centrifuged at top speed for 1 min after each wash to pellet the beads. The beads were then resuspended in sample buffer and heated to 99 C for 10 min before SDS-PAGE. Gels were subjected to Western blotting analysis using 1:1000 anti-GFP mouse monoclonal antibody (Roche). Secondary horseradish peroxidase-conjugated mouse (Cell Signaling Technology, Hitchin, UK) antibody was used at a concentration of 1:5000, and blots were developed using the ECLplus chemiluminescence system (Amersham, Little Chalfont, UK).

Retroviral vectors and vector production

The γ-retroviral vector backbone was derived from the vector SERS11.SF.gp91s.iGM.W (37). Using *Xba*I and *Sal*I, the cassette containing gp91phox-IRES-ΔMGMT-GFP was exchanged by the full-length coding region of wild-type ALADIN fused to enhanced cyan fluorescent protein at its carboxy or amino terminus resulting in an expression of CFP-ALADIN or ALADIN-CFP in the subsequently transduced HeLa cells. Cell-free viral supernatants were generated by transient cotransfection of HEK293T cells as described elsewhere (38). HeLa target cells were plated in 1.5-cm dishes and were transduced with retroviral titers. Forty-eight hours after transduction, the cells were subcultured. Single-cell colonies were obtained by single-cell sorting into 96-well plates with a flow cytometer, cultured, and analyzed by fluorescence microscopy.

Confocal microscopy

SK-N-SH cells were plated in eight-well glass chamber slides at a concentration of 5,000–10,000 cells per well and transiently transfected (as above) with pEGFP-*AAAS* or pcDNA3.1-*FTH1*-V5-HIS or both vectors, and 48 h after transfection, cells were fixed in 3.7% formaldehyde followed by permeabilization with 0.1% (vol/vol) Triton X-100. To minimize nonspecific cross-reactivity, cells were incubated in buffer A (3% BSA, 10% normal donkey serum in PBS) for 45 min before incubation with 1:200 anti-V5 mouse antibody (Invitrogen) in buffer A for 90 min. Cells were then incubated with secondary Cy3-conjugated donkey antimouse antibody (Jackson ImmunoResearch, New Market, UK) diluted 1:100 in buffer A. Vectashield (Vector Laboratories Inc., Peterborough, UK) fluorescent mounting medium containing 4′,6-diamidino-2-phenylindole (DAPI) was added to the slides, and immunofluorescence was visualized using a Zeiss LSM 510 laser scanning confocal microscope. The following excitation/emission conditions were used in separate channels with either the ×40 or ×63 oil immersion objective: DAPI 364/475–525 nm, GFP 488/505–530 nm, and Cy3 543/560–600 nm.

FLIM-FRET

All FLIM-FRET experiments were undertaken in HeLa cells stably expressing CFP-ALADIN and were transfected with C-terminal YFP-tagged FTH1 or with C-terminal YFP-tagged NUP88. Twenty-four hours after transfection, the cells were fixed for 10 min using 3.7% formaldehyde and embedded in Vectashield mounting medium. The transfection efficiency was shown to be 90–95% before performing the FLIM-FRET measurements.

Fluorescence lifetime measurements were performed by wide-field time-domain FLIM as described previously (39) with minor changes. Briefly, an excitation wavelength of 440 nm was used. Images were recorded on a Zeiss Axiovert S100TV with a ×63 1.4 NA oil immersion objective through a 455LP dichroic mirror and a D480/40m emission filter (Chroma filter set 31044v2). The fluorescence decay curves were recorded by 18 images with increasing delay times (step 0.5 nsec) after the excitation laser pulse with a camera binning of 4 × 4 and an exposure time of 200–400 msec for each image. The laser power was reduced by ND filters to avoid photobleaching during the acquisition. Images were background corrected by subtracting the mean value of a region without any fluorescence signal. The fluorescence lifetime of CFP was calculated by tail fitting of the decay curve for each pixel according to a single-exponential decay function: $I(t) = A \cdot e^{-t/\tau}$. Additionally, we analyzed the fluorescence decay of a whole cell by a double-exponential decay function $I(t) = A_1 \cdot e^{-t/\tau 1} + A_2 \cdot e^{-t/\tau 2}$ with I being the measured intensity at a time point t, the preexponential factors A_1 and A_2, and the fluorescent lifetimes $\tau 1$ and $\tau 2$. The mean lifetime τ_m was calculated as a weighted average according to: $\tau_m = (A_1\tau_1^2 + A_2\tau_2^2)/(A_1\tau_1 + A_2\tau_2)$.

Significance of the fluorescence lifetime shifts was analyzed using the two-tailed Mann-Whitney *U* test. *P* values < 0.0001 were considered as significant.

PARP cleavage

Human neuroblastoma SH-SY5Y cells were used for these studies in view of their greater transfection efficiency. Cells were plated in six-well plates and allowed to reach 60–70% confluency before being transiently transfected with either pEGFP-*AAAS*, pcDNA3.1-*FTH1* or pEGFP-*AAAS* and pcDNA3.1-*FTH1* using Lipofectamine and Plus reagent (Invitrogen), according to the manufacturer's instructions. At 24 h after transfection, cells were incubated in serum-free medium containing 1 mM H_2O_2 for 30 min before the medium was replaced with fresh serum-containing medium in all cells (40). After overnight recovery at 37 C, cells were lysed and analyzed via Western analysis, using PARP polyclonal antibody at 1:1000 (Cell Signaling Technology) and GAPDH at 1:2000 (Santa Cruz Bio-

technology, Santa Cruz, CA). PARP cleavage was quantified using densitometric analysis from four representative experiments and normalized to GAPDH. Student's *t* test was used for statistical analysis.

Acknowledgments

We thank Dr. Marina Doufexis who provided technical advice and support for the bacterial two-hybrid work.

Address all correspondence and requests for reprints to: Professor Adrian J. L. Clark, Centre for Endocrinology, William Harvey Research Institute, John Vane Science Centre, Charterhouse Square, London EC1M 6BQ, United Kingdom. E-mail: a.j.clark@qmul.ac.uk.

Disclosure Summary: B.K., D.A.P., J.P.C., M.L., and A.J.L.C. have nothing to declare. H.L.S. was supported by a Clinical Training Fellowship from St. Bartholomew's and The Royal London Charitable Foundation Research Advisory Board (JRB XMML) and a Wellcome Trust Clinical Training Fellowship (GR072616MA). A.H. was supported by a grant of the German Research Foundation (HU 895/3-4) and K.K. by a MeDDrive grant form the Medical Faculty of the Technical University Dresden.

References

1. **Clark AJ, Weber A** 1998 Adrenocorticotropin insensitivity syndromes. Endocr Rev 19:828–843
2. **Prpic I, Huebner A, Persic M, Handschug K, Pavletic M** 2003 Triple A syndrome: genotype-phenotype assessment. Clin Genet 63:415–417
3. **Grant DB, Barnes ND, Dumic M, Ginalska-Malinowska M, Milla PJ, von Petrykowski W, Rowlatt RJ, Steendijk R, Wales JH, Werder E** 1993 Neurological and adrenal dysfunction in the adrenal insufficiency/alacrima/achalasia (3A) syndrome. Arch Dis Child 68:779–782
4. **Huebner A, Elias LL, Clark AJ** 1999 ACTH resistant syndromes. J Pediatr Endocrinol Metab 12:277–293
5. **Tullio-Pelet A, Salomon R, Hadj-Rabia S, Mugnier C, de Laet MH, Chaouachi B, Bakiri F, Brottier P, Cattolico L, Penet C, Bégeot M, Naville D, Nicolino M, Chaussain JL, Weissenbach J, Munnich A, Lyonnet S** 2000 Mutant WD-repeat protein in triple-A syndrome. Nat Genet 26:332–335
6. **Handschug K, Sperling S, Yoon SJ, Hennig S, Clark AJ, Huebner A** 2001 Triple A syndrome is caused by mutations in AAAS, a new WD-repeat protein gene. Hum Mol Genet 10:283–290
7. **Huebner A, Kaindl AM, Braun R, Handschug K** 2002 New insights into the molecular basis of the triple A syndrome. Endocr Res 28:733–739
8. **Smith TF, Gaitatzes C, Saxena K, Neer EJ** 1999 The WD repeat: a common architecture for diverse functions. Trends Biochem Sci 24:181–185
9. **Storr HL, Clark AJ, Priestley JV, Michael GJ** 2005 Identification of the sites of expression of triple A syndrome mRNA in the rat using in situ hybridisation. Neuroscience 131:113–123
10. **Dreger M, Bengtsson L, Schöneberg T, Otto H, Hucho F** 2001 Nuclear envelope proteomics: novel integral membrane proteins of the inner nuclear membrane. Proc Natl Acad Sci USA 98:11943–19948
11. **Cronshaw JM, Krutchinsky AN, Zhang W, Chait BT, Matunis MJ** 2002 Proteomic analysis of the mammalian nuclear pore complex. J Cell Biol 158:915–927
12. **Cronshaw JM, Matunis MJ** 2003 The nuclear pore complex ALADIN is mislocalized in triple A syndrome. Proc Natl Acad Sci USA 100:5823–5827
13. **Krumbholz M, Koehler K, Huebner A** 2006 Cellular localization of 17 natural mutant variants of ALADIN protein in triple A syndrome: shedding light on an unexpected splice mutation. Biochem Cell Biol 84:243–249
14. **Peter M, Ameer-Beg SM, Hughes MK, Keppler MD, Prag S, Marsh M, Vojnovic B, Ng T** 2005 Multiphoton-FLIM quantification of the EGFP-mRFP1 FRET pair for localization of membrane-receptor-kinase interactions. Biophys J 88:1224–1237
15. **Biskup C, Zimmer T, Benndorf K** 2004 FRET between cardiac Na^+ channel subunits measured wit a confocal microscope and a streak camera. Nat Biotechnol 22:220–224
16. **D'Angelo MA, Hetzer MW** 2008 Structure, dynamics and function of nuclear pore complexes. Trends Cell Biol 18:456–466
17. **Oliver FJ, de la Rubia G, Rolli V, Ruiz-Ruiz MC, de Murcia G, Murcia JM** 1998 Importance of poly(ADP-ribose) polymerase and its cleavage in apoptosis. Lesson from an uncleavable mutant. J Biol Chem 273:33533–33539
18. **Nicholson DW, Ali A, Thornberry NA, Vaillancourt JP, Ding CK, Gallant M, Gareau Y, Griffin PR, Labelle M, Lazebnik YA, Munday NA, Raju SM, Smulson ME, Violeta TT Yamin, Yu VL, Miller DK** 1995 Identification and inhibition of the ICE/CED-3 protease necessary for mammalian apoptosis. Nature 376:37–43
19. **Cai CX, Linsenmayer TF** 2001 Nuclear translocation of ferritin in corneal epithelial cells. J Cell Sci 114:2327–2334
20. **Cai CX, Birk DE, Linsenmayer TF** 1998 Nuclear ferritin protects DNA from UV damage in corneal epithelial cells. Mol Biol Cell 9:1037–1051
21. **Linsenmayer TF, Cai CX, Millholland JM, Beazley KE, Fitch JM** 2005 Nuclear ferritin in corneal epithelial cells:tissue-specific nuclear transport and protection from UV-damage. Prog Retin Eye Res 24:139–159
22. **Millholland JM, Fitch JM, Cai CX, Gibney EP, Beazley KE, Linsenmayer TF** 2003 Ferritoid, a tissue-specific nuclear transport protein for ferritin in corneal epithelial cells. J Biol Chem 278:23963–23970
23. **Surguladze N, Patton S, Cozzi A, Fried MG, Connor JR** 2005 Characterisation of nuclear ferritin and mechanism of nuclear import. Biochem J 388:731–740
24. **Thompson K, Fried M, Ye Z, Boyer P, Connor J** 2002 Regulation, mechanisms and proposed function of ferritin translocation to cell nuclei. J Cell Sci 115(Pt 10):2165–2177
25. **Thompson K, Menzies S, Muckenthaler M, Torti FM, Wood T, Torti SV, Hentze MW, Beard J, Connor J** 2003 Mouse brains deficient in H-ferritin have normal iron concentration but a protein profile of iron deficiency and increased evidence of oxidative stress. J Neurosci Res 71:46–63
26. **Powers JM, Pei Z, Heinzer AK, Deering R, Moser AB, Moser HW, Watkins PA, Smith KD** 2005 Adreno-leukodystrophy: oxidative stress of mice and men. J Neuropathol Exp Neurol 64:1067–1079
27. **Huebner A, Mann P, Rohde E, Kaindl AM, Witt M, Verkade P, Jakubiczka S, Menschikowski M, Stoltenburg-Didinger G, Koehler K** 2006 Mice lacking the nuclear pore complex protein ALADIN show female infertility but fail to develop a phenotype resembling human triple A syndrome. Mol Cell Biol 26:1879–1887
28. **Reshmi-Skarja S, Huebner A, Handschug K, Finegold DN, Clark AJ, Gollin SM** 2003 Chromosomal fragility in patients with triple A syndrome. Am J Med Genet A 117A:30–36
29. **Hirano M, Furiya Y, Asai H, Yasui A, Ueno S** 2006 $ALADIN^{I482S}$ causes selective failure of nuclear protein import and hypersensitivity to oxidative stress on triple A syndrome. Proc Natl Acad Sci USA 103:2298–2303
30. **Kiriyama T, Hirano M, Asai H, Ikeda M, Furiya Y, Ueno S** 2008 Restoration of nuclear-import failure caused by triple A syndrome and oxidative stress. Biochem Biophys Res Commun 374:631–634
31. **Goizet C, Catargi B, Tison F, Tullio-Pelet A, Hadj-Rabia S, Pujol F,**

Lagueny A, Lyonnet S, Lacombe D 2002 Progressive bulbospinal amyotrophy in triple A syndrome with AAAS gene mutation. Neurology 58:962–965

32. **Rosen DR, Siddique T, Patterson D, Figlewicz DA, Sapp P, Hentati A, Donaldson D, Goto J, O'Regan JP, Deng HX, Rahmani Z, Krizus A, McKenna-Yasek D, Cayabyab A, Gaston S, Berger R, Tanzi R, Halperin J, Herzfeldt B, Van den Bergh R, Hung WY, Bird T, Deng G, Mulder D, Smyth C, Laing N, Soriano E, Pericak-Vance M, Haines J, Rouleau G, Gusella J, Horvitz H, Brown R** 1993 Mutations in Cu/Zn superoxide dismutase gene are associated with familial amyotrophic lateral sclerosis. [Erratum (1993) 364:362] Nature 362:59–62
33. **Reynolds A, Laurie C, Mosley RL, Gendelman HE** 2007 Oxidative stress and the pathogenesis of neurodegenerative disorders. Int Rev Neurobiol 82:297–325
34. **Huebner A, Kaindl AM, Knobeloch KP, Petzold H, Mann P, Koehler K** 2004 The triple A syndrome is due to mutations in ALADIN, a novel member of the nuclear pore complex. Endocr Res 30:891–899
35. **Gackowski D, Rozalski R, Siomek A, Dziaman T, Nicpon K, Klimarczyk M, Araszkiewicz A, Olinski R** 2008 Oxidative stress and oxidative DNA damage is characteristic for mixed Alzheimer disease/vascular dementia. J Neurol Sci 266:57–62
36. **Doufexis M, Storr HL, King PJ, Clark AJ** 2007 Interaction of the melanocortin 2 receptor with nucleoporin 50: evidence for a novel pathway between a G-protein-coupled receptor and the nucleus. FASEB J 21:4095–4100
37. **Moreno-Carranza B, Gentsch M, Stein S, Schambach A, Santilli G, Rudolf E, Ryser MF, Haria S, Thrasher AJ, Baum C, Brenner S, Grez M** 2009 Transgene optimization significantly improves SIN vector titers, gp91(phox) expression and reconstitution of superoxide production in X-CGD cells. Gene Ther 16:111–118
38. **Demaison C, Parsley K, Brouns G, Scherr M, Battmer K, Kinnon C, Grez M, Thrasher AJ** 2002 High-level transduction and gene expression in hematopoietic repopulating cells using a human immunodeficiency virus type 1-based lentiviral vector containing an internal spleen focus forming virus promoter. Hum Gene Ther 13: 803–813
39. **Lorenz M** 2009 Visualizing protein-RNA interactions inside cells by fluorescence resonance energy transfer. RNA 15:97–103
40. **Bailey TA, Kanuga N, Romero IA, Greenwood J, Luthert PJ, Cheetham ME** 2004 Oxidative stress affects the junctional integrity of retinal pigment epithelial cells. Invest Ophthalmol Vis Sci 45:675–684